Proceedings of the 7th International Symposium on Cavitation
CAV2009 – Paper No.32
August 17-22, 2009, Ann Arbor, Michigan, USA

Comparison of cavitation erosion rate with liquid impingement erosion rate

Shuji Hattori
Graduate School of Engineering,
University of Fukui
Fukui-shi, Japan

Makoto Takinami
Graduate School of Engineering,
University of Fukui
Fukui-shi, Japan

Tomoaki Otani
University of Fukui
Fukui-shi, Japan

ABSTRACT

Both cavitation erosion and liquid impingement erosion are phenomena that can cause pipe wall thinning in power plants. The Code for Power Generation Facilities, Rules on Pipe Wall Thinning Management, was published by the JSME (Japan Society of Mechanical Engineers) in 2005. The code says that cavitation erosion shall be prevented either in the design stage or by daily inspection. On the other hand, liquid impingement erosion can occur in any location where a working fluid attacks a pipe wall at high flow velocities. Therefore, it is very important to evaluate the amount of erosion by liquid impingement for pipe steels quantitatively from the viewpoint of aging management. In this study, we carried out both cavitation erosion and liquid impingement erosion tests, and clarified the relation between the two erosion rates. As a result, we found that the erosion rate by cavitation increases in proportion with the 5.2th to 6.8th power of the flow velocity and that by liquid impingement with the 6.0th to 7.4th power. Moreover, a good correlation was obtained between erosion rates by cavitation and by liquid impingement. We also discussed the erosion mechanism with SEM photography, and proposed an erosion model.

INTRODUCTION

Both cavitation erosion and liquid impingement erosion are phenomena that can cause pipe wall thinning in power plants. The Code for Power Generation Facilities, Rules on Pipe Wall Thinning Management [1], was published by the JSME (Japan Society of Mechanical Engineers) in 2005. The code says that cavitation erosion shall be prevented either in the design stage by a daily inspection. On the other hand, liquid impingement erosion can occur at locations where a working fluid attacks a pipe wall at high flow velocity. The liquid impingement damage occurs downstream of elbows and T-tubes, and just behind orifices and valves. The most effective parameter for liquid impingement erosion is the flow velocity. The impact load increases in proportion with the first to second power of the velocity and the erosion rate with the 4th to 5th power. Therefore, it is possible to prevent the occurrence of liquid impingement erosion by operating power plants at low flow velocities, but it is not realistic from the viewpoint of power generation efficiency. Many studies of liquid impingement erosion have been carried out for steam turbines [2], but very few for pipe wall thinning. It is very important to evaluate the amount of erosion by liquid impingement for pipe wall thinning quantitatively from the viewpoint of aging management. Heymann [3] indicated that the processes of liquid impingement erosion and cavitation erosion are very similar. In our laboratory, about one thousand test data of cavitation erosion have been accumulated [4], which will be available for comparison with liquid impingement erosion data.

In this study, we carried out erosion tests of pipe steels by

Table 1: Chemical compositions

(mass%)

Material	C	Si	Mn	V	P	S	Cu	Ni	Mo	Cr	Al	Fe	Ti
Al	-	0.06	-	0.01	-	-	0.01	-	-	-	Bal	0.12	0.01
S15C	0.16	0.21	0.45	-	0.01	0.016	0.01	0.02	-	0.05	-	Bal	-
SUS304	0.06	0.2	1.67	-	0.034	0.027	-	8.0	-	18.73	-	Bal	-
STPA24	0.12	0.35	0.47	0.002	0.012	0.004	0.02	0.02	0.93	2.12	0.002	Bal	0.001

Table 2: Physical and mechanical properties

Material	Density kg/m^3	Tensile strength MPa	Vickers hardness HV0.2
Al	2.71×10^3	95	38
S15C	7.81×10^3	441	145
SUS304	7.93×10^3	694	171
STPA24	7.72×10^3	630	216

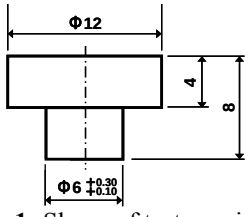

Figure 1: Shape of test specimen

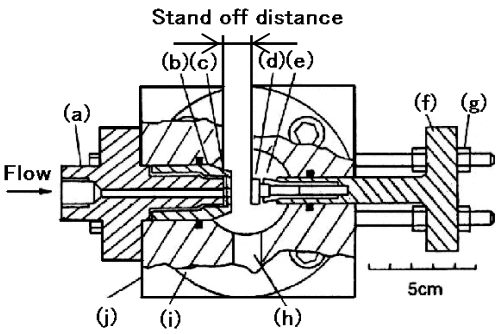

Figure 2: Test apparatus

liquid impingement and by cavitation, and clarified the relation between both erosion rates in order to predict the erosion rate by liquid impingement based on the rate by cavitation. We also observed the erosion process with SEM photography, and we discussed the erosion mechanism.

TEST MATERIALS AND TEST METHOD

The test materials are pure aluminum to determine the optimum stand-off distance according to ASTM G134-95 [5], S15C (0.15% carbon steel, equivalent to carbon pipe steel), SUS304 (austenite stainless steel, equivalent to stainless pipe steel) and STPA24 (alloy steel for pipes) for the erosion tests. The chemical compositions and the physical and mechanical properties of these materials are listed Tables 1 and 2, respectively. The shape of the test specimen, as shown in Figure 1, is 12 mm in diameter and 4 mm in thickness. The test specimen was mirror-finished by buffing after being polished with emery paper up to grade #1200.

Figure 2 shows the cavitating liquid jet test chamber which is specified in the ASTM G134-95 standard [5]. The test liquid is tap water kept at 35±2 degree Celsius. The cavitation erosion tests were carried out in a test chamber, and the flow velocity was determined by controlling upstream and downstream pressures (both were absolute pressures) at a constant cavitation number of 0.025. The flow velocity V is given by the following equation

$$V = \sqrt{\frac{2(p_u - p_d)}{\rho}} \qquad (1)$$

where ρ is the liquid density kg/m^3, p_u the upstream pressure and p_d the downstream pressure (absolute pressure MPa). The cavitation number σ shows the tendency for cavitation to occur in flowing system of liquids, and is defined by the following equation

$$\sigma = \frac{p_d - p_v}{p_u - p_d} \qquad (2)$$

where p_v is the vapor pressure (absolute pressure MPa). For the cavitation erosion test, the test specimen was removed periodically at predetermined time intervals, and weighed with a precision balance (sensitivity of 0.01 mg) after cleaning with acetone in an ultrasonic bath.

As mentioned above, since the existing studies for liquid impingement erosion are very few regarding pipe wall thinning, liquid impingement erosion tests were carried out in the same test chamber. The flow velocity was calculated by Eq. (1) with controlling only the upstream pressure at a constant down stream pressure of 0.1 MPa (atmospheric pressure). The liquid jet impinges on the specimen surface in air. Test liquid and temperature were the same as in the cavitation erosion tests. For the liquid impingement erosion tests, the test specimen was removed periodically at predetermined time intervals, and the profile of the eroded surface was measured with a noncontact – type profilometer (resolution of 0.1 μm and measurement interval of 4 μm) after cleaning with acetone in an ultrasonic bath.

In the cavitation erosion tests, the amount of erosion reaches a maximum at the location where most bubbles collapse. Therefore, a preliminary test was carried out to determine the optimum stand-off distance. Figure 3 shows the relation between the stand-off distance and the mass loss of the pure aluminum specimen after a test of 30 minutes. Since the amount of erosion reached the maximum at a stand-off distance of 10mm, the optimum stand-off distance was determined to be 10 mm. Moreover, since it has become clear from another

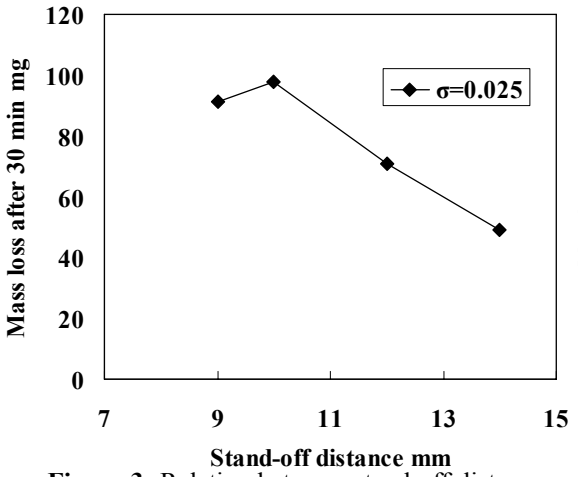

Figure 3: Relation between stand-off distance and mass loss of Al

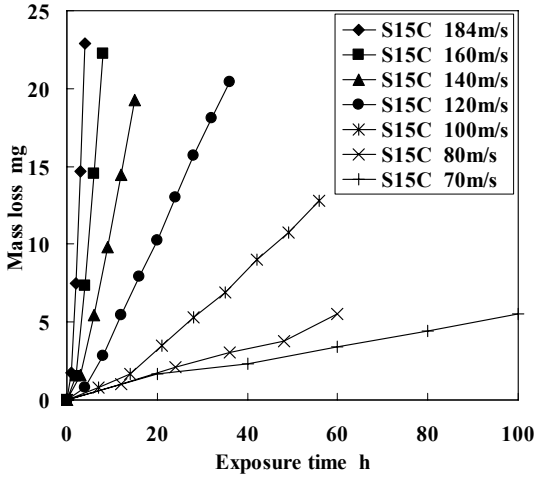

Figure 4: Mass loss curves of S15C (cavitation)

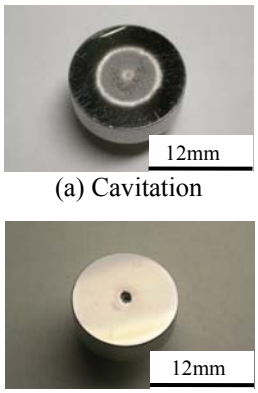

(a) Cavitation

(b) Liquid impingement

Figure 5: Eroded specimen

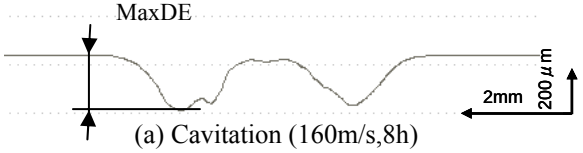

(a) Cavitation (160m/s,8h)

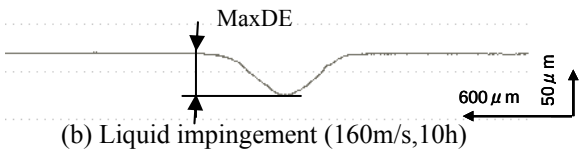

(b) Liquid impingement (160m/s,10h)

Figure 6: Profiles of eroded surface

study in our laboratory that the impact energy of liquid impingement does not depend on the stand-off distance, the optimum stand-off distance for the liquid impingement erosion test was also set to 10 mm.

TEST RESULTS AND DISCUSSION

Figure 4 shows the mass loss curves of S15C in the cavitation test. The mass loss curves show an incubation stage where plastic deformation successively occurs on the material surface, an acceleration stage with a gradual increase in erosion, and a maximum rate stage with a rapid increase [5]. Figure 5 shows an example of eroded specimens. The specimen surface after the cavitation erosion test (a) was found to be eroded in ring form with a diameter of 6.5 mm. The specimen surface after the liquid impingement erosion test (b) was found to be eroded over a small area with a diameter of 1mm. Figure 6 also shows examples of eroded surface profiles. The profile after the cavitation erosion test (a) was eroded in a W-shaped form with a depth of 200 μm after 8 hours at 160m/s. The profile after the liquid impingement erosion test (b) was eroded in a conical form with a depth of 50μm after 10 hours at 160 m/s. The MaxDE is defined as the maximum depth of erosion, as shown in Figure 6.

Since the MaxDE is very important than mass loss for pipe wall thinning, the MaxDE was obtained by measuring the surface profile of an eroded specimen after the cavitation erosion test. We assumed that the MaxDE increases in proportion to the mass loss, and calculated the MaxDE from the mass loss curves at predetermined time intervals. Figure 7(a) shows the MaxDE curves of S15C which were calculated from Figure 4. The incubation period is longer and the slope of the maximum rate period is smaller at lower flow velocities. Especially, the MaxDE at 70m/s is about 25 μm after 100hr.

As shown in Figure 5, the eroded area by liquid impingement is much smaller than that by cavitation, and it was difficult to measure the mass loss precisely. Therefore, the MaxDE was obtained with a profilometer by measuring the eroded surface at predetermined time intervals. Figure 7(b) shows the MaxDE curves of S15C by liquid impingement. These curves also show the incubation, the acceleration and the

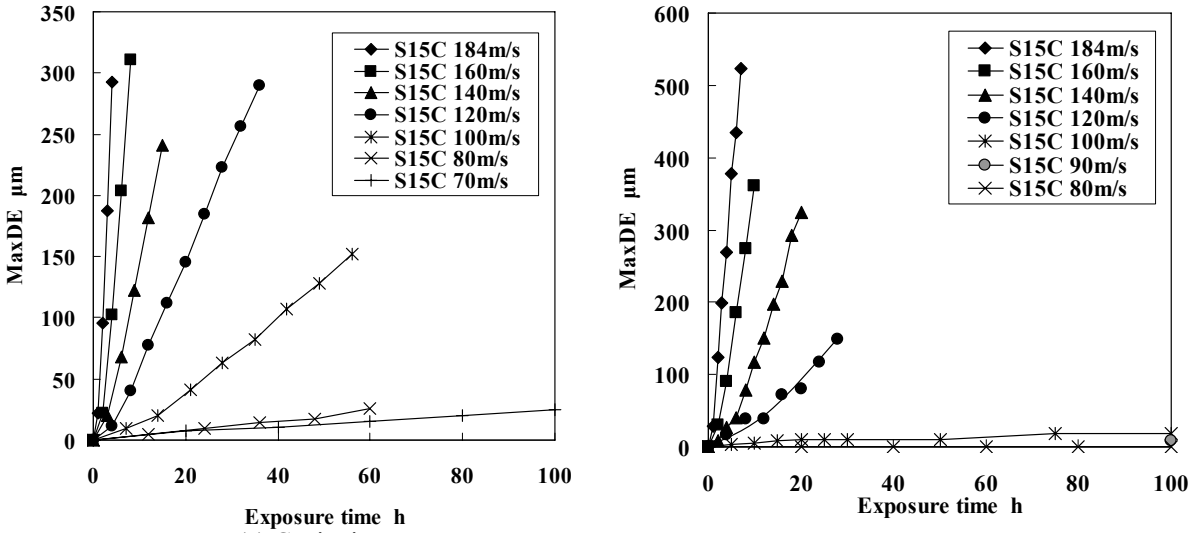

(a) Cavitation (b) Liquid impingement

Figure 7: MaxDE curves of S15C

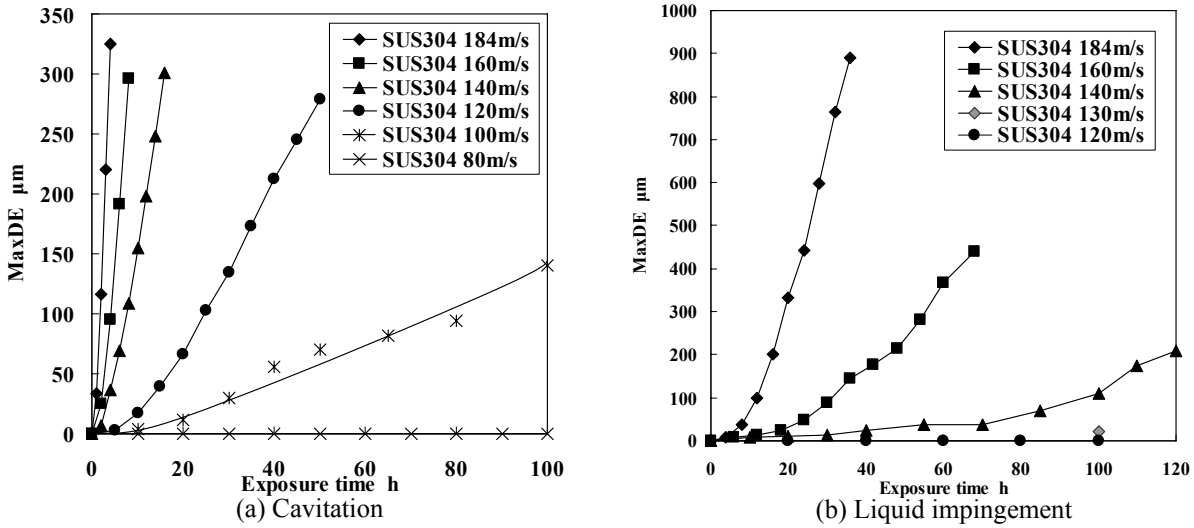

(a) Cavitation (b) Liquid impingement

Figure 8: MaxDE curves of SUS304

maximum erosion rate stages as shown in Figure 7(a), and we can see the similarity of the erosion behaviors by cavitation and by liquid impingement. The behavior of the MaxDE curves for liquid impingement is very similar to that for cavitation at 184m/s down to 140m/s. Erosion, however, did not occur at 80m/s in liquid impingement erosion test.

The test results for SUS304, STPA24, and S15C were evaluated by calculating the MaxDE from the mass loss in the cavitation erosion test, and by measuring the MaxDE directly for the liquid impingement erosion test. Figure 8 shows the MaxDE curves of SUS304 for cavitation and for liquid impingement. For SUS304, erosion rates of the MaxDE curves by cavitation are different from that by liquid impingement. For example, it takes 4 hours for cavitation and 20 hours for liquid impingement until a MaxDE reached 300μm to 350μm at a flow velocity of 184m/s.

Figure 9 shows the MaxDE curves of STPA24 for cavitation and for liquid impingement. The behavior of the MaxDE curves for cavitation is very similar to that for liquid impingement at higher flow velocities of 184m/s down to 140m/s. This is also true for the behavior of the MaxDE curves of S15C. On the other hand, the erosion rates for cavitation are higher than for liquid impingement at lower flow velocities.

Figure 10 shows the flow velocity dependence of the MaxDER (maximum depth of erosion rate) for each material. The MaxDER is defined as the increment of the MaxDE in the maximum erosion rate stage divided by the respective test time interval. The MaxDER by cavitation (Figure 10(a)) increases in proportion with the 5.2th to 6.8th power of the flow velocity. This agrees with an increase of the erosion rate by cavitation in proportion with the 4th to 9th power of the flow velocity [6]. The MaxDER by liquid impingement (Figure 10(b)) also increases in proportion with the 6.0th to 7.4th power of the flow velocity. This is higher than the 4th to 5th power of the flow velocity [1]. In this way, we find that the flow velocity dependences of the MaxDER by cavitation and by liquid impingement are very similar. In addition, the threshold velocity for the onset of erosion was obtained in this study.

Figure 11 shows the relation between the MaxDER by cavitation and by liquid impingement for each test material. A

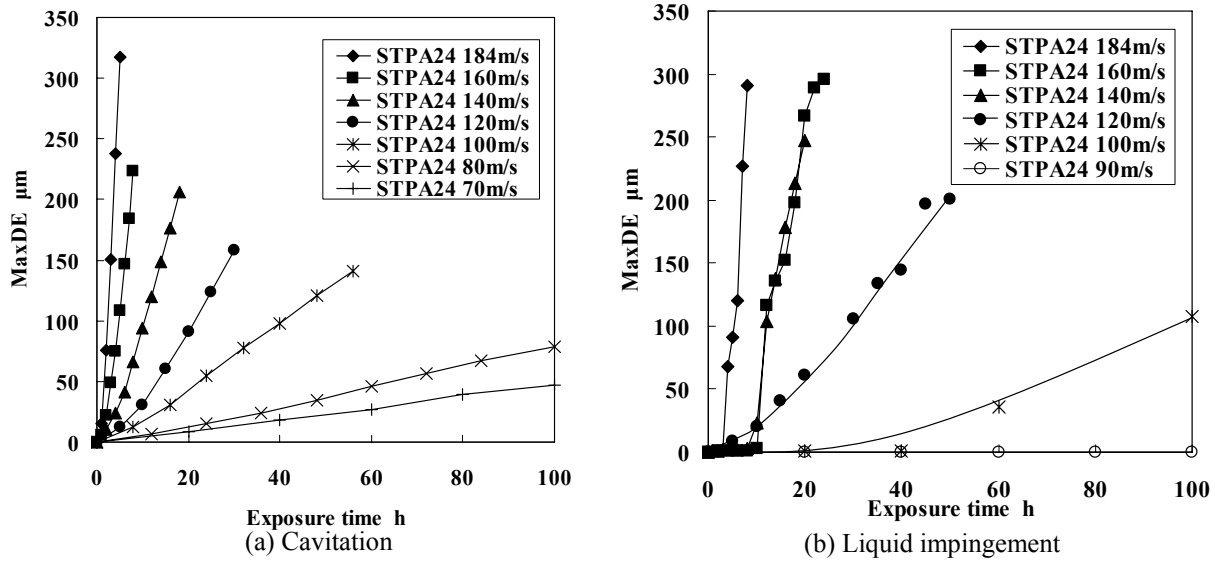

(a) Cavitation (b) Liquid impingement

Figure 9: MaxDE curves of STPA24

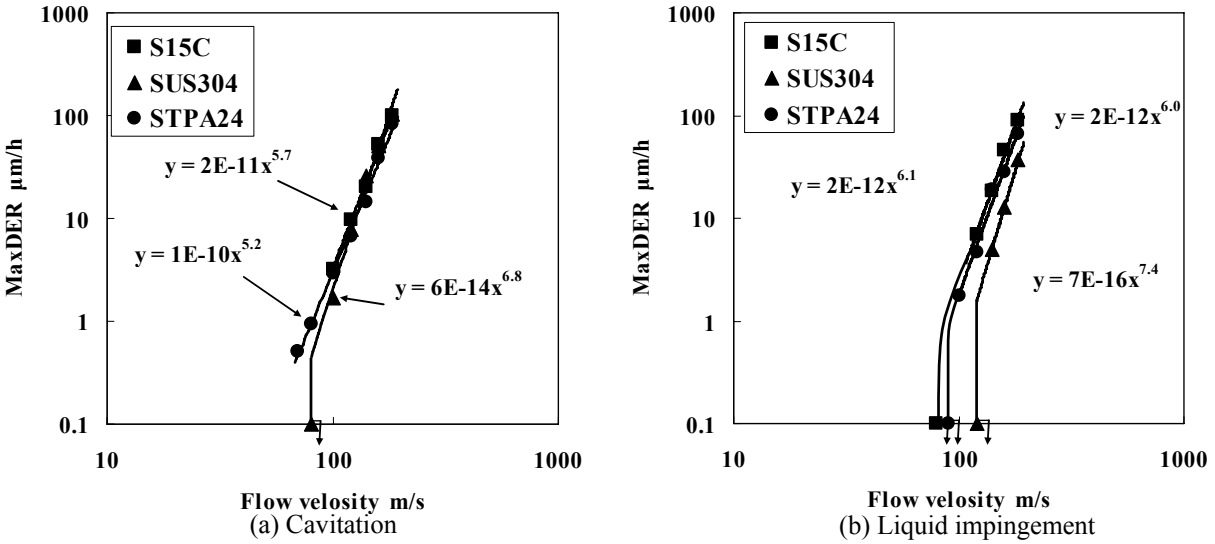

(a) Cavitation (b) Liquid impingement

Figure 10: Flow velocity dependence of MaxDER

good correlation was obtained for the MaxDER caused by cavitation and by liquid impingement, and it is possible to approximate them by straight lines passing through the origin. The MaxDER of SUS304, however, is much smaller than that of S15C and STPA24. Generally a higher hardness material has lower erosion rate. However, SUS304 is a high work-hardening material during static tensile test compared to the other steels. We consider that the hardness of SUS304 increases higher during liquid impingement test, because the test produces smaller loads than the cavitation test. Therefore, the erosion rate of SUS304 in liquid impingement becomes lower than those of the other steels. Figure 12 shows the distribution of the impact loads obtained with a sensor, which was developed in our laboratory [7]. Several thousand counts were detected for small impact loads and several counts for large impact loads. Regarding the maximum, an impact load of 21N was detected for cavitation (a) at 184m/s, and a maximum impact load of 7N for liquid impingement at 200m/s. Thus, we conclude that the difference in impact loads has an effect on the work hardening of SUS304.

Figure 13 shows the eroded surface of SUS304 by vibratory cavitation at the same location, which was observed in a scanning electron microscopy (SEM). Cavitation erosion in a cavitating liquid jet apparatus proceeds similarly to that in a vibratory apparatus [8]. After 45 minutes (Figure 13(a)), plastic deformation occurred inside crystal grains by cavitation and accumulated at grain boundaries. After 3 hr (Figure 13(b)), crack-like grooves began to occur in the highly deformed area along grain boundaries. After 4 hr (Figure 13(c)), material removal (erosion) occurred in the grain. After 5 hr (Figure 13(d)), the erosion extended across a wide area inside the grain.

Figure 14 shows the eroded surface of SUS304 by liquid impingement at the same location, which was observed by a different type of scanning electron microscopy (reflecting electron image) from that used in Figure 13 (secondary electron image). Attention should be paid to the differences in the black-and-white images between these two Figures. The erosion process by liquid impingement is similar to that by cavitation. Plastic deformation occurred inside crystal grains, and crack-like grooves appeared along grain boundaries, where material removal occurred. From Figures 13 and 14, we conclude that the erosion mechanisms between cavitation and liquid impingement are very similar.

Figure 15 shows a schematic model of the erosion over the cross section based on the observation of the eroded surface. Figure 15(a) corresponds to the initial stage of erosion. The original surface is repeatedly exposed to the collapse of cavitation bubbles or to liquid impingement. Therefore, plastic deformation of the material surface occurs by shock waves of the liquid impingement or by micro jets in the cavitation bubble collapses. Since liquid impingement or cavitation bubble collapse repeatedly acts on the deformed area, the area gradually expands, and plastic deformation accumulates at the crystal grain boundaries. Since the material surface is plastically deformed, swelled portions appear at the crystal grain boundaries. These swelled parts produce a step relative to the adjacent grain with less plastic deformation and cause a high stress concentration, resulting in fatigue crack initiation as shown in Figure 15(c). Figure 15(d) shows that erosion easily occurs at a crack initiation site. Figure 15(d) corresponds to the SEM photograph after 4 hours for vibratory cavitation in Figure

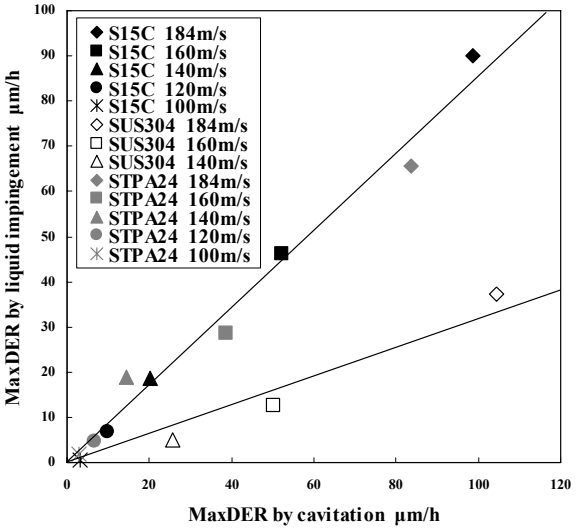

Figure 11: Relation between MaxDER by cavitation and by liquid impingement

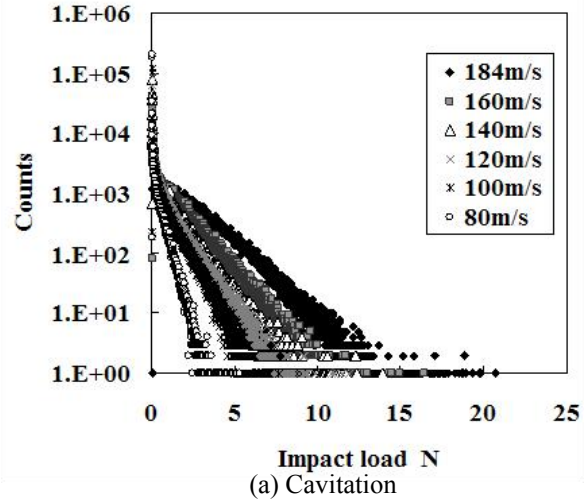

(a) Cavitation

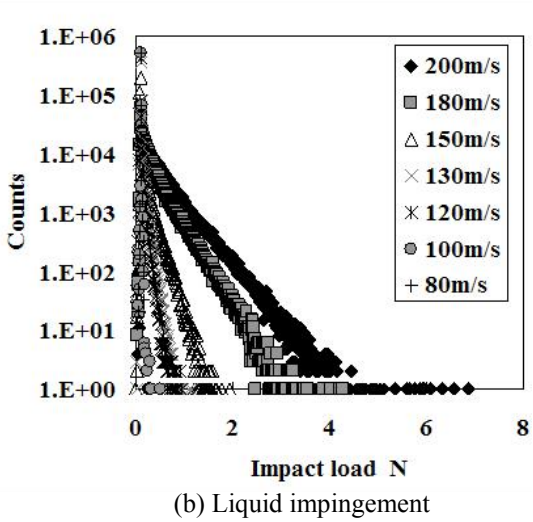

(b) Liquid impingement

Figure 12: Distribution of impact loads

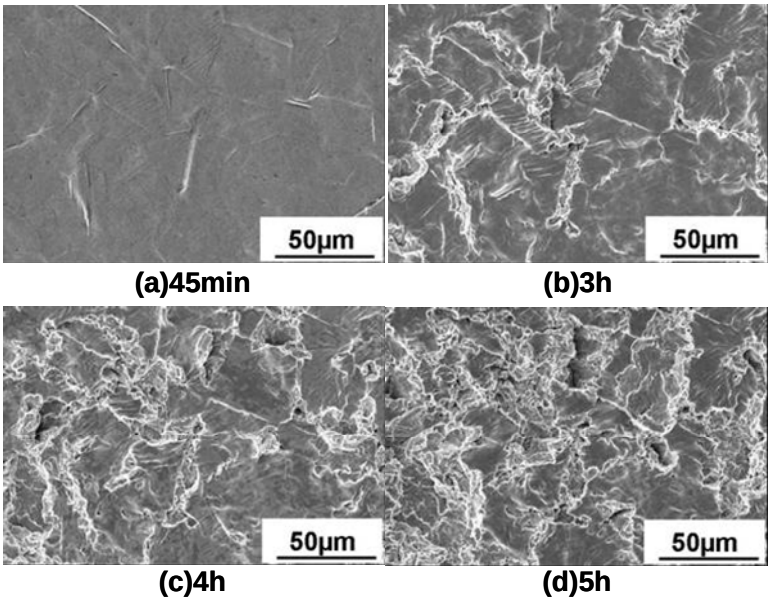

Figure 13: Erosion surface (SUS304, cavitation)

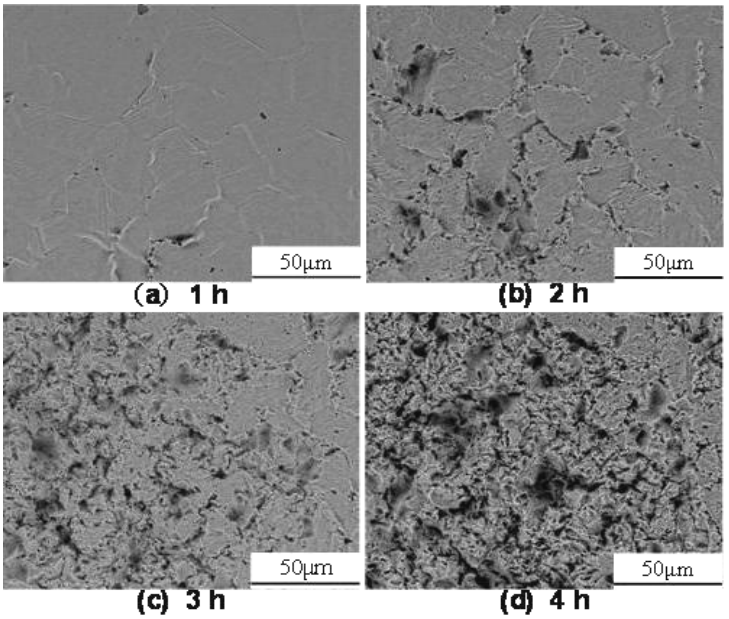

Figure 14: Erosion surface (SUS304, liquid impingement)

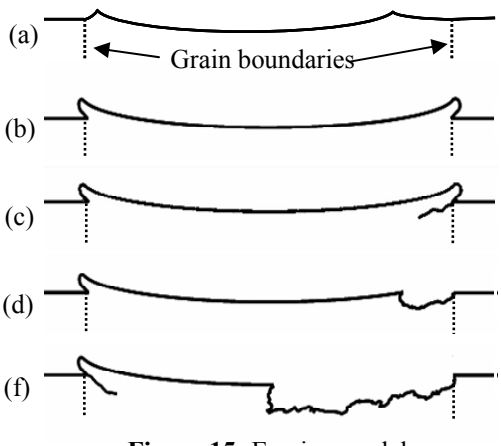

Figure 15: Erosion model

13, and to that after 3 hours for liquid impingement in Figure 14. Figure 15(e) shows a further eroded surface. Thus, Figures 15(a) to 15(c) correspond to the erosion in its incubation stage, and Figures 15(d) and 15(c) correspond to that in the acceleration stage.

CONCLUSION

(1) Erosion both by cavitation and by liquid impingement goes through similar incubation, acceleration and maximum rate stages.

(2) Since the relation of the maximum depth erosion rate (MaxDER) for liquid impingement and cavitation is approximated in both cases by a straight line passing through the origin, the correlation between these erosion rates is very high.

(3) The erosion mechanism by liquid impingement and by cavitation proceed due to fatigue. That is, swelled parts appear by plastic deformation at the crystal grain boundaries and the same areas produce high stress concentrations, resulting in fatigue crack initiation and material removal.

(4) Since the correlation between both forms of erosion is very high, many cavitation erosion data are now available for the prediction of liquid impingement erosion.

ACKNOWLEDGMENTS

The authors would like to acknowledge the financial support from both Institute of Nuclear Safety System, Incorporated, and Nuclear and Industrial Safety Agency, Ministry of Economy, Trade and Industry. The project is on the Technical Information Basis of Aging Management for nuclear power plants.

REFERENCES

[1] The Japan Society of Mechanical Engineers 2005, "Codes for Power Generation Facilities," *Rules on Pipe Wall Thinning Management*, JSME S CA1-2005, 48-70

[2] Brunton, J. H. and Rochester M. C. 1979, "Erosion of Solid Surfaces by the Impact of Liquid Drops," *Treatise on Material Science and Technology*, 16, 185-248,

[3] Heymann, F. H. 1992, "Liquid Impingement Erosion," *ASM Handbook*, 18, 221-232

[4] Hattori, S., Ishikura, R. and Zhang, Q. 2004, "Construction of database on cavitation erosion and analyses of carbon steel data," *Wear,* 257, 1022-1029

[5] ASTM Designation G134-95 2005, *Annual Book of ASTM Standards*, 576-588

[6] Preece, C. M. 1979, "Cavitation Erosion," *Treatise on Material Science and Technology*, 16, 249-308

[7] Hattori, S., Mori, H. and Okada, T. 1998, "Quantitative Evaluation of Cavitation Erosion," *ASME*, 120, 179-185

[8] Hattori, S., Maekawa, N. and Kuwabara, M. 2001, "Comparison of Cavitation Erosion between Cavitating Jet and Vibratory Methods Specified in ASTM Standard," *Transaction of the Japan Society of Mechanical Engineers*, A, 655, 67, 470-475